Lifetime Evaluation of Grid-Connected PV Inverters Considering Panel Degradation Rates and Installation Sites

Ariya Sangwongwanich, *Student Member, IEEE*, Yongheng Yang, *Member, IEEE*, Dezso Sera, *Senior Member, IEEE*, and Frede Blaabjerg, *Fellow, IEEE*

***Abstract*—Lifetime of Photovoltaic (PV) inverters is affected by the installation sites related to different solar irradiance and ambient temperature profiles (also referred to as mission profiles). In fact, the installation site also affects the degradation rate of the PV panels and, thus, long-term energy production and reliability. Prior-art lifetime analysis in PV inverters has not yet investigated the impact of PV panel degradations. This paper, thus, evaluates the lifetime of PV inverters considering panel degradation rates and mission profiles. Evaluations have been carried out on PV systems installed in Denmark and Arizona. The results reveal that the PV panel degradation rate has a considerable impact on the PV inverter lifetime, especially in the hot climate (e.g., Arizona), where the panel degrades at a faster rate. In that case, the PV inverter lifetime prediction can be deviated by 54%, if the impact of PV panel degradations is not taken into account.**

***Index Terms*—Degradation, lifetime, mission profile, Monte Carlo method, PV inverters, reliability.**

I. Introduction

PHOTOVOLTAIC (PV) technology has a potential to become a major energy source in the near future, and has experienced a high growth rate during the last decades [1]. As more PV systems have been installed and connected to the grid, their reliability and lifetime are gaining more and more attention [2]–[4]. With the recent technology, the lifetime of PV panels is normally warranted at 20–25 years, whereas the PV inverter lifetime is usually limited to less than 15 years [5]. Thus, the PV inverter has been reported as one of the most critical components that cause failures in the entire PV systems [6], [7]. For grid-connected PV systems, the cost associated with the PV inverter failure is around 59% of the total system cost [8]. Therefore, the lifetime prediction of PV inverters plays a crucial role in terms of the operational cost assessment and, thus, design for reliability.

Lifetime of grid-connected PV inverters can be significantly influenced by their operating conditions, which will affect the thermal loading of the power devices [9]–[11]. This could be due to different control strategies of the PV inverters (e.g., maximum power point tracking (MPPT) operation, reactive power injection, and limiting power injection) [12]–[15], but also the installation sites (more specific, solar irradiance and ambient temperature profiles, also referred to as mission profiles). Studies in [16]–[19] have revealed that the installation location has a considerable impact on the reliability and lifetime of PV inverters. This is due to the fact that the mission profile of the PV inverters (i.e., solar irradiance and ambient temperature) varies according to its installation sites. For instance, the installation site at the geographical location close to the equator (e.g., South America and Africa) will normally have a relatively high average solar irradiance level throughout a year. In those regions, only small seasonal variations in the solar irradiance profile is usually observed. In contrast, some installation sites located in the northern part of the world (e.g., Scandinavia countries) usually have a relatively low average solar irradiance level during winter, and the solar irradiance profile can vary considerably during a year [20]. Similar tendency is also applied to the ambient temperature profile of the installation site. The solar irradiance and ambient temperature have a direct impact on the PV power production (due to the PV panel characteristic), which will in return contribute to the thermal loading of the PV inverter due to the power losses dissipated in the power devices [e.g., insulated-gate bipolar transistor (IGBT)]. In addition, the ambient temperature of the installation site will also have a direct impact on the thermal loading (i.e., the junction temperature) of the power device. Consequently, the PV inverter lifetime will be affected by the variations in the solar irradiance and ambient temperature of the installation sites. Hence, mission profiles are normally considered in the PV inverter lifetime prediction and reliability assessment.

However, the prior-art work did not take the impact of PV panel degradations into account in the lifetime evaluation. In other words, it is usually assumed that the PV power production and the thermal loading of the PV inverter are repeated yearly for certain installation sites. Therefore, the life consumption

Manuscript received November 11, 2016; revised January 17, 2017; accepted February 28, 2017. Date of publication March 3, 2017; date of current version November 2, 2017. This work was supported in part by the European Commission within the European Union's Seventh Frame-work Program (FP7/2007–2013) through the SOLAR-ERA.NET Transnational Project (PV2.3-PV2GRID), by Energinet.dk (ForskEL, Denmark, Project 2015-1-12359), and in part by the Research Promotion Foundation (RPF, Cyprus, Project KOINA/SOLAR-ERA.NET/0114/02). Recommended for publication by Associate Editor Y. Xing. *(Corresponding author: Yongheng Yang).*

The authors are with the Department of Energy Technology, Aalborg University, Aalborg DK-9220, Denmark (e-mail: ars@et.aau.dk; yoy@et.aau.dk; des@et.aau.dk; fbl@et.aau.dk).

Color versions of one or more of the figures in this paper are available online at http://ieeexplore.ieee.org.

Digital Object Identifier 10.1109/TPEL.2017.2678169

(LC) of the PV inverters, which indicates how much the life of inverter has been consumed, is normally determined from, e.g., an annual mission profile. Then, the LC is accumulated with a linear approximation by assuming a constant yearly LC, and the lifetime of the PV inverter is determined. However, this assumption is not very accurate in practical applications, as it is well known that the PV panels degrade during operation. More precisely, the aged PV panels will produce less energy than the newly installed ones under the same solar irradiance and ambient temperature conditions [21]–[25]. This implies that the thermal loading and thereby the LC of the PV inverter will be reduced over time (under the same mission profile), according to the panel degradation rate. In fact, the PV panel degradation rate is influenced by climate conditions, which also varies with the location of the installation sites [25]–[31]. For instance, the PV panel tends to degrade faster under dry and hot climate conditions, where a degradation rate of 1%/year has been measured [30]. In this case, the assumption of a constant yearly LC, which only considers the thermal loading in the first year, will lead to a significant underestimate of the PV inverter lifetime.

According to the above discussions, it is obvious that the PV panel degradation has a direct impact on the long-term thermal loading of the PV inverter and, thus, its lifetime prediction. In order to represent a more realistic operating condition and improve the lifetime estimation accuracy of the PV inverter, the degradation rates of the PV panels at different installation locations have to be taken into account [32]. This paper thus proposes a lifetime evaluation of the PV inverters considering the panel degradation rates and mission profiles. In the proposed solution, the impact of the PV panel degradation is taken into account during the mission profile translation process, offering a more realistic interpretation of the long-term PV inverter thermal loading. Two installation sites in Denmark and Arizona, which have different mission profiles and panel degradation characteristics, are considered and a mission profile-based lifetime evaluation has been applied. Then, the reliability assessment based on the Monte Carlo simulation is carried out, where the parameter variations are taken into account in the lifetime evaluation process. By doing so, the lifetime of the PV inverter (component- and system-level) can be obtained in terms of statistical value (e.g., B_x lifetime). The predicted lifetime have shown a considerable impact of the PV panel degradation on the PV inverter lifetime, especially in Arizona, due to a high panel degradation rate.

The rest of this paper is organized as follows: the description of the case study is provided in Section II. Then, the mission profile-based lifetime estimation is presented in Section III. The lifetime evaluation and the reliability assessment of the case study are carried out in Sections IV and V, respectively. Finally, concluding remarks are given in Section VI.

II. Description of the Case Study

A. System Description

The BP365 PV panel is used in this study, where the panel characteristic at the standard test condition (STC) is given in Table I [33]. In this case, a PV string consists of 15 PV panels, and 6 PV strings are connected in parallel in order to achieve the rated power around 6 kW. Then, a two-stage PV system consisting of a boost dc–dc converter and a full-bridge dc–ac inverter (PV inverter) is employed as the interface between the PV panels and the ac grid [34]. The system configuration is shown in Fig. 1, and its parameters are given in Table II. Regarding the power devices, five 600V/30A IGBT devices from a leading manufacturer are used [35], and the cooling system (e.g., heat sink sizing) is designed to ensure the maximum junction temperature of 120 °C at the rated operating condition.

TABLE I
Parameters of the BP 365 Solar PV Panel at the STC [33]

Panel rated power	$P_{\text{mpp}} = 65$ W
Voltage at the maximum power point	$V_{\text{mpp}} = 17.6$ V
Current at the maximum power point	$I_{\text{mpp}} = 3.69$ A
Open-circuit voltage	$V_{\text{OC}} = 21.7$ V
Short-circuit current	$I_{\text{SC}} = 3.99$ A

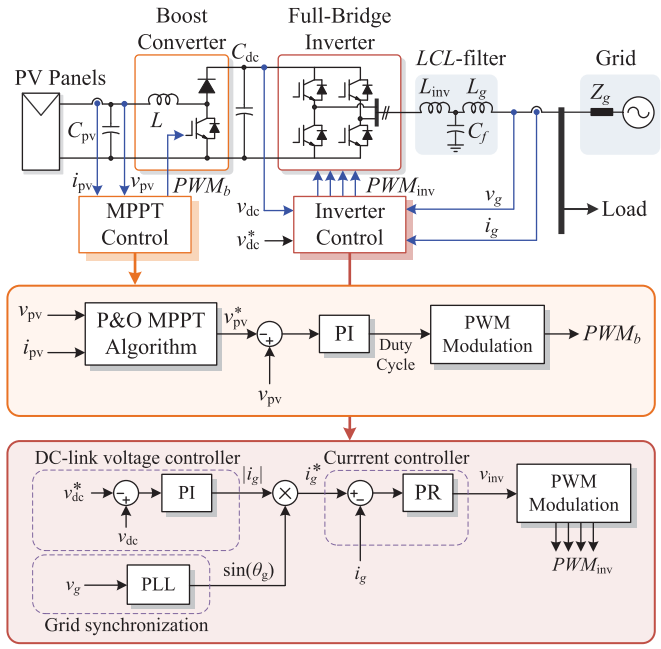

Fig. 1. System configuration and control structure of a two-stage single-phase grid-connected PV system (PI—proportional integral, PR—proportional resonant, PLL—phase locked loop, PWM - pulse width modulation).

TABLE II
Parameters of the Two-Stage Single-Phase PV System (Fig. 1)

PV inverter rated power	6 kW
Boost converter inductor	$L = 1.8$ mH
PV-side capacitor	$C_{\text{pv}} = 1000\ \mu$F
DC-link capacitor	$C_{\text{dc}} = 1100\ \mu$F
LCL-filter	$L_{\text{inv}} = 4.8$ mH, $L_{\text{g}} = 2$ mH, $C_f = 4.3\ \mu$F
Switching frequency	Boost converter: $f_b = 16$ kHz, Full-Bridge inverter: $f_{\text{inv}} = 8$ kHz
dc-link voltage	$v^*_{\text{dc}} = 450$ V
Grid nominal voltage (RMS)	$V_g = 230$ V
Grid nominal frequency	$\omega_0 = 2\pi \times 50$ rad/s

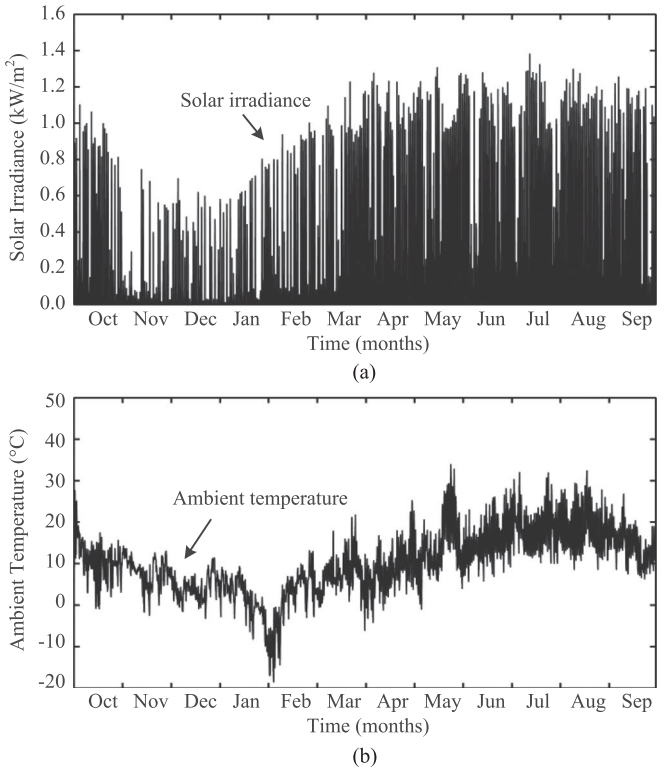

Fig. 2. Yearly mission profiles from the installation site in Denmark with a sampling rate of 5 min/sample: (a) Solar irradiance and (b) ambient temperature.

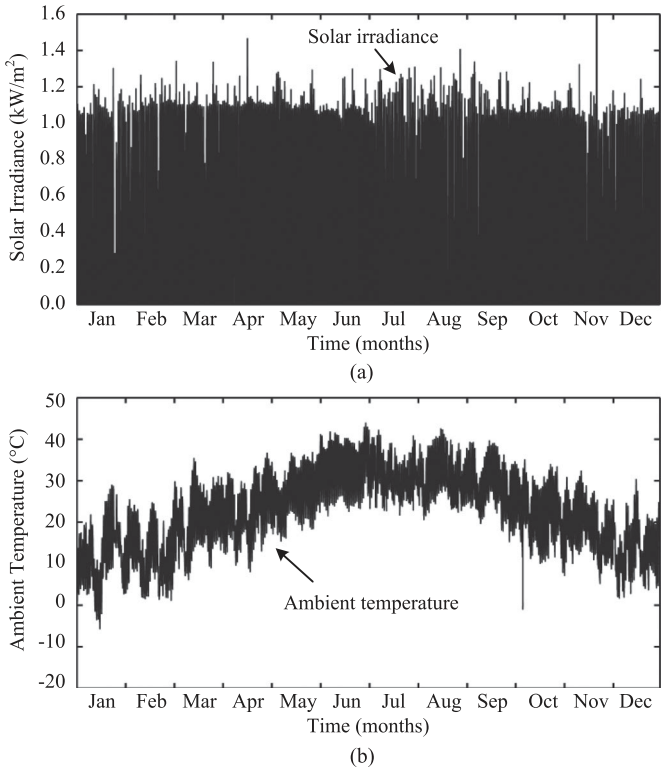

Fig. 3. Yearly mission profiles from the installation site in Arizona with a sampling rate of 5 min/sample: (a) Solar irradiance and (b) ambient temperature.

This two-stage configuration is widely used in residential PV systems [36], where the MPPT operation is implemented in the boost converter. Then, the PV inverter (i.e., a full-bridge inverter) delivers the extracted power to the ac grid by regulating the dc-link voltage $v_{\rm dc}$ to be constant [37]. In order to do so, the current controller is acting to regulate the grid current i_g according to a reference given by the dc-link voltage controller. Notably, a phased-locked loop (PLL) is also implemented to extract the phase angle of the grid in order to determine the reference grid current.

B. Mission Profile of the PV Systems

In order to evaluate the lifetime of the PV inverter under real operating conditions, a mission profile, which is a representation of the operating condition of the system, is needed [11]. In the case of PV applications, the solar irradiance and ambient temperature are considered as mission profiles, since the PV power production is strongly dependent on the two parameters. As discussed previously, the mission profile of the PV system can vary considerably according to the geographical locations of installation. In this paper, two mission profiles recorded in Denmark and Arizona shown in Figs. 2 and 3 are used. It can be seen from the mission profiles that the average solar irradiance level in Arizona is constantly high throughout the year, whereas it is relatively low in Denmark from November to February. The ambient temperature in Denmark also varies in a wide range, where the minimum value reaches -18 °C. In contrast, the temperature profile in Arizona remains positive throughout the year with the maximum value of 44 °C.

The mission profiles in Figs. 2 and 3 represent two different scenarios where the PV systems are installed in: an average low solar irradiance and ambient temperature location (i.e., Denmark); and an average high solar irradiance and ambient temperature location (i.e., Arizona). It can be expected that the PV power production in Arizona will be higher than in Denmark. However, the PV panel degradation rates at the two installed locations differ significantly, which will have a considerable impact on the long-term PV power production.

C. Degradation Rate of the PV Panels

As mentioned previously, the long-term PV power production is not only determined by the mission profile of the PV system, but also on the degradation rate of the PV panels. Studies in [25] and [27] have indicated that the PV panel degradation rate varies considerably according to the installation location. These large variations in the degradation rate are mainly influenced by different climate conditions of the installation sites (e.g., ambient temperature and humidity) [25], [27]. A study of the collected real-field data has been carried out in [24]–[26]. In general, the PV panels tend to degrade faster under dry and hot climate conditions compared to the PV panels installed in cold climate conditions.

In addition, the panel degradation characteristics should also be taken into account when considering the PV panel

degradation impacts. According to the study in [38], the degradation characteristic of the PV panel can be varied according to the PV panel failure mode (e.g., degradation mechanism). For instance, an encapsulant discoloration, which is one of the most commonly-reported failure modes in PV panels, usually leads to a linear degradation of PV panels where the PV power production decreases linearly over time. On the other hand, a nonlinear degradation behavior can be observed in some PV panels with solder bond fatigue and solder bond failure. This is also dependent on the PV panel technologies, where the thin-film technology has been witnessed with a higher tendency of nonlinear degradation behaviors [38]. However, modeling the PV panel degradation in details is very challenging, since different climate conditions and PV panel technology can result in different failure modes [21]. Moreover, different failure modes may also have cross-effects on the other failure mechanisms. This can lead to a much more complicated system which may not be suitable (or possible) for a long-term simulation (e.g., yearly mission profiles).

Alternatively, the PV panel degradation rate can also be determined from real-field measurements, as it has been done in [23], [39], and [28]. In that case, a linear degradation characteristic is usually assumed, where the degradation profile is obtained from the real-field measured data [22], [28]. In fact, this is actually suitable for many practical cases, where the PV panel is not often characterized (e.g., measure output power at the STC) during operation. For instance, it has been reported that the measurement of PV panel output power at the STC is usually done once during the entire life span, resulting in a limited number of data points [26]. In the worst case, only one measurement is performed after several years of operation, and the PV panel output power (at the STC) from the measurements is compared with the datasheet value to determine the power difference. In that case, it makes sense to apply the linear degradation model for the PV panels. However, it is worth to mention that the accuracy of the degradation model is compromised with this approach due to the simplified linear model. Some practical aspects such as nonuniform degradation rate over the entire PV plant or partial shading effect cannot be taken into account. Nevertheless, it offers a simple but practical solution for a long-term simulation without requiring a large set of measurement data or detailed model of the PV panel. Thus, this approach is suitable to be applied with the mission profile-based lifetime evaluation used in this paper. Moreover, this linear degradation modeling approach has been widely applied to estimate the long-term PV energy yield in the design phase (e.g., to calculate the levelized cost of PV energy) [40], [41].

In light of the above discussions, a linear degradation model based on the measurement data will be considered in this paper. In this study, the degradation rate of 0.15%/year in Denmark and 1%/year in Arizona are used, according to the field measurements in [29]–[31]. The yearly degradation profile of the PV panels at these locations is illustrated in Fig. 4. Nevertheless, it should be mentioned that the mission profile-based lifetime evaluation presented in this paper can also be generally applied to any arbitrary degradation characteristic (e.g., linear degradation, exponential degradation, or from real-data measurements).

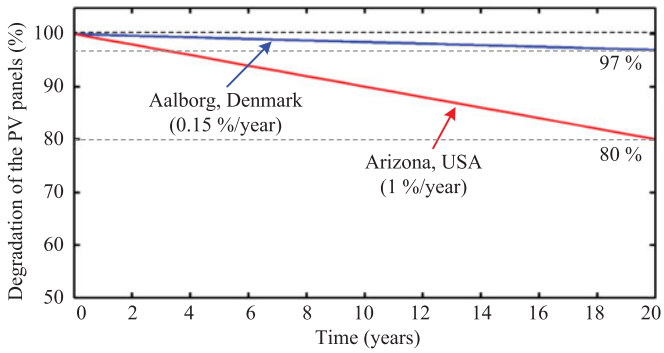

Fig. 4. Degradation profiles of the PV panels installed in Denmark and Arizona with the degradation rate of 0.15%/year and 1%/year, respectively.

This will be further addressed in the mission profile translation process in Section III.

III. Mission Profile-Based Lifetime Estimation

A procedure is required to estimate the lifetime of the PV inverter under certain mission profiles. This is because the lifetime model of the critical components in the PV inverter (e.g., power device) usually relates to the temperature variations [4]. Therefore, the mission profile should be first translated into the thermal loading of the PV inverter (i.e., device junction temperature T_j) [20]. Then, the required information in the lifetime model (e.g., mean junction temperature $T_{\rm jm}$, cycle amplitude ΔT_j, and cycle period $t_{\rm on}$) can be extracted from the thermal loading profile by using a counting algorithm (e.g., rainflow method). After that, a specific lifetime model can be applied, and the lifetime can be estimated. The diagram of this process is depicted in Fig. 5.

A. Mission Profile Translation to Thermal Loading

As discussed previously, the mission profiles should be translated into the thermal loading of the PV inverter. In fact, the junction temperature variations are related to the power losses $P_{\rm loss}$ dissipated in the power device and the cooling system. Thus, there are intermediate steps between this translation, which relates to the power generated at each stage.

First, the available PV power of the PV arrays $P_{\rm mpp}$ is determined from the solar irradiance and ambient temperature profiles by using the panel characteristic model [42]. By doing so, the time-varying available PV power profile (according to the applied mission profile) can be obtained. Then, the proposed lifetime evaluation approach determines the actual PV output power from the PV arrays $P_{\rm pv}$ (i.e., input power of the boost converter) by multiplying the available PV power $P_{\rm mpp}$ with the panel degradation rate. This is in contrast to the previous work, where the available PV power $P_{\rm mpp}$ is directly interpreted as the actual PV output power from the PV arrays $P_{\rm pv}$ during the entire operation. Notably, the panel degradation rate is also a time-varying profile (see Fig. 4), which can either be modeled by a mathematical function (e.g., linear function, exponential function) or obtained from a real-field measured data. In other

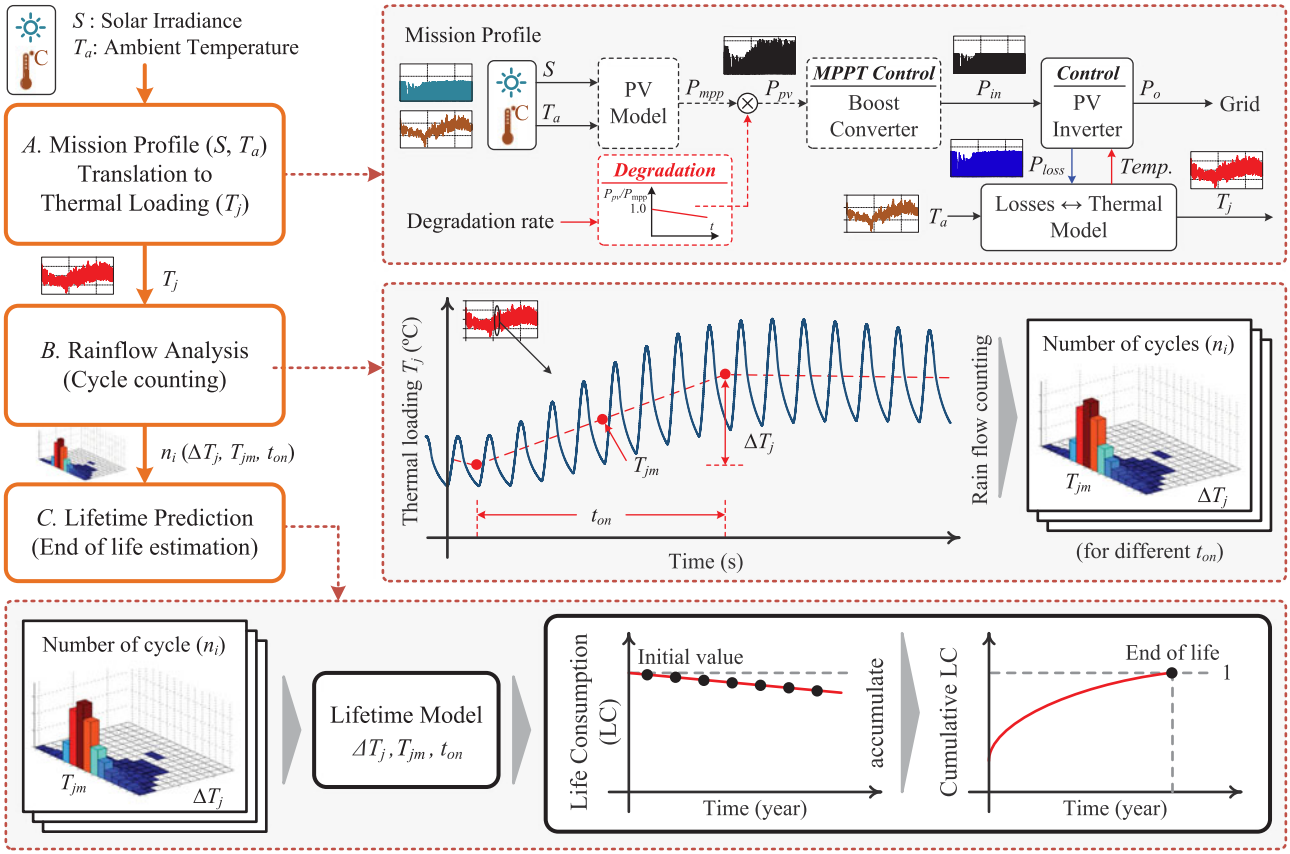

Fig. 5. Flow diagram of the mission profile-based lifetime evaluation of PV inverters considering the PV panel degradation [20].

words, any arbitrary PV panel degradation profile can be applied to this approach.

Afterwards, the power losses P_{loss} dissipated in the power devices can be calculated by taking the MPPT operation efficiency (99%) and the PV inverter efficiency into account. Once the power losses P_{loss} are calculated, the device junction temperature profile T_j can be obtained from the thermal model of the power device (e.g., the Cauer model or the Foster model). This thermal model also considers the ambient temperature of the PV inverter, as it affects the power device junction temperature variations (e.g., mean junction temperature). Notably, this process is implemented by using a look-up table generated from the power device electrical characteristic (i.e., conduction and switching behaviors) and the thermal impedance given in the datasheet in order to assist a long-term simulation (e.g., yearly profiles) [20].

B. Cycle Counting using Rainflow Analysis

The junction temperature variation obtained from the previous step is an irregular profile, according to the mission profile. In order to apply such a junction temperature profile to the lifetime model, a counting algorithm such as a rainflow analysis is needed [10]. The rainflow counting algorithm is widely used in the lifetime and stress analysis related to the thermal cycling, which is the case for the power devices used. It can divide the irregular profile (like the thermal loading) into several regular cycles, and categorize them according to the cycle amplitude, its average value, and the cycle period. Thus, by applying the rainflow counting algorithm to the device junction temperature profile, the number of cycles n_i at a certain cycle amplitude ΔT_j, mean junction temperature T_{jm}, and cycle period t_{on} can be obtained (see Fig. 5).

C. Lifetime Model of the PV Inverters (Power devices)

The lifetime estimation of the entire PV inverter requires in-depth knowledge of multiple subjects, since the components (e.g., capacitors and IGBT) in the PV system can have cross effects of the reliability among each other. In order to simplify the analysis, the lifetime of the power device is only considered here. The lifetime model of the IGBT is given as

$$N_f = A \times (\Delta T_j)^{\alpha} \times (ar)^{\beta_1 \Delta T_j + \beta_0} \times \left[\frac{C + (t_{\text{on}})^{\gamma}}{C+1}\right] \times \exp\left(\frac{E_a}{k_b \times T_{\text{jm}}}\right) \times f_d \quad (1)$$

where N_f is the number of cycles to failure [43]. The mean junction temperature T_{jm}, cycle amplitude ΔT_j, and cycle period t_{on} are considered as inputs for this lifetime model, whereas the other parameters are given in Table III.

TABLE III
PARAMETERS OF THE LIFETIME MODEL OF AN IGBT MODULE [43]

Parameter	Value	Experimental condition
A	3.4368×10^{14}	
α	-4.923	$64\ \text{K} \leq \Delta T_j \leq 113\ \text{K}$
β_1	-9.012×10^{-3}	
β_0	1.942	$0.19 \leq ar \leq 0.42$
C	1.434	
γ	-1.208	$0.07\ \text{s} \leq t_{\text{on}} \leq 63\ \text{s}$
f_d	0.6204	
E_a	0.06606 eV	$32.5\ ^\circ\text{C} \leq T_j \leq 122\ ^\circ\text{C}$
k_B	8.6173324×10^{-5} eV/K	

The LC is then calculated by using the Miner's rule [10] as

$$\text{LC} = \sum_i \frac{n_i}{N_{fi}} \tag{2}$$

where n_i is the number of cycles (obtained from the rainflow analysis) for a certain T_{jm}, ΔT_j, and t_{on}, whereas N_{fi} is the number of cycles to failure calculated from (1) at that specific stress condition. The LC can be used to indicate how much the life of the power device is consumed (or damaged) during operation. For instance, if the number of cycles n_i is counted from an annual mission profile, the LC calculated in (2) will represent a yearly LC of the power device. The lifetime of the power device is then determined when the LC accumulates to unity, which is when the device reaches its end of life.

IV. LIFETIME EVALUATION (CASE STUDY)

In this section, the lifetime evaluation discussed in Section III is applied to the case study. The junction temperature variations and the LC of the power device are compared.

A. Junction Temperature Variations

The junction temperature variation is a consequence of the power device loading. In this regards, the impact of PV panel degradations can be observed in the junction temperature variations in the PV inverters. Figs. 6 and 7 show the mean junction temperatures T_{jm} and the cycle amplitudes ΔT_j of the PV inverters at the two installation sites, respectively. Due to the higher average irradiance level in Arizona, the mean junction temperature T_{jm} of the PV inverter in Arizona is in general higher than in Denmark. However, the mean junction temperature T_{jm} of the PV inverter in Arizona reduces significantly after 5 years of operation, due to the high degradation rate of the PV panels. It can be seen from Fig. 6 that the mean junction temperature in Arizona is approximately 3 °C lower compared to the first year, whereas the reduction in the mean junction temperature is very small in Denmark. Similarly, the cycle amplitude of the junction temperature ΔT_j is also reduced significantly after 5 years of operation for the PV inverter installed in Arizona. According to the above results, the degradation rate of the PV panel has a strong influence on the long-term device junction temperature and, thus, the PV inverter lifetime.

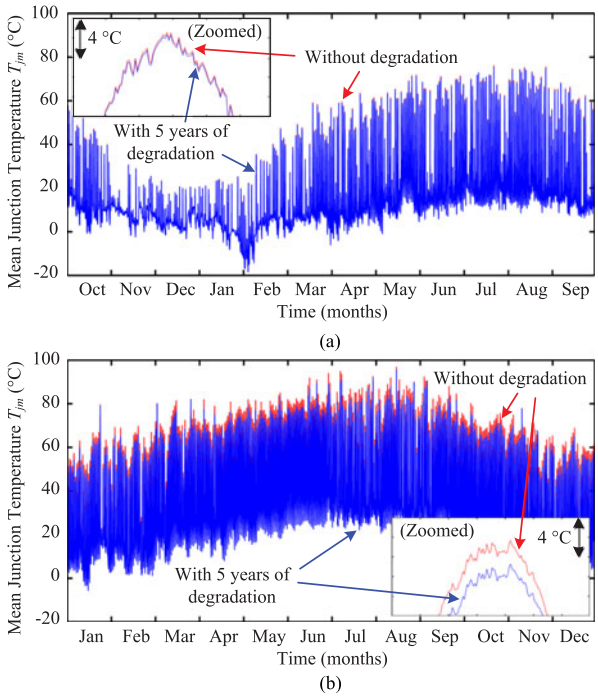

Fig. 6. Mean junction temperature T_{jm} of the power device under a yearly mission profile in: (a) Denmark and (b) Arizona.

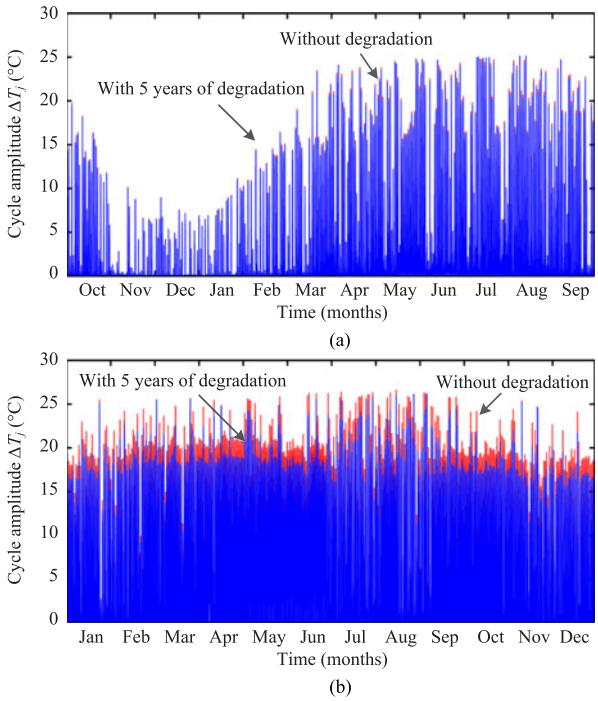

Fig. 7. Cycle amplitude ΔT_j of the device junction temperature under a yearly mission profile in: (a) Denmark and (b) Arizona.

B. Lifetime Evaluation

From the extracted thermal loading profiles, the lifetime evaluation can be applied according to Fig. 5. The yearly LC of the power device is calculated for an operation of 20 years in order to observe the impact of the panel degradation in the long-term LC. It can be seen from Fig. 8 that the yearly LC of the PV

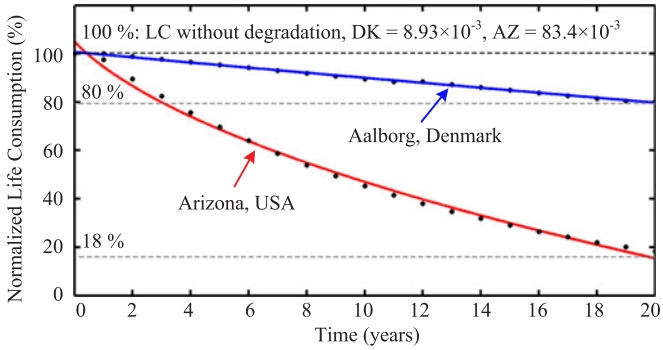

Fig. 8. Normalized yearly LC of the power device during 20 years of operation in Denmark and Arizona.

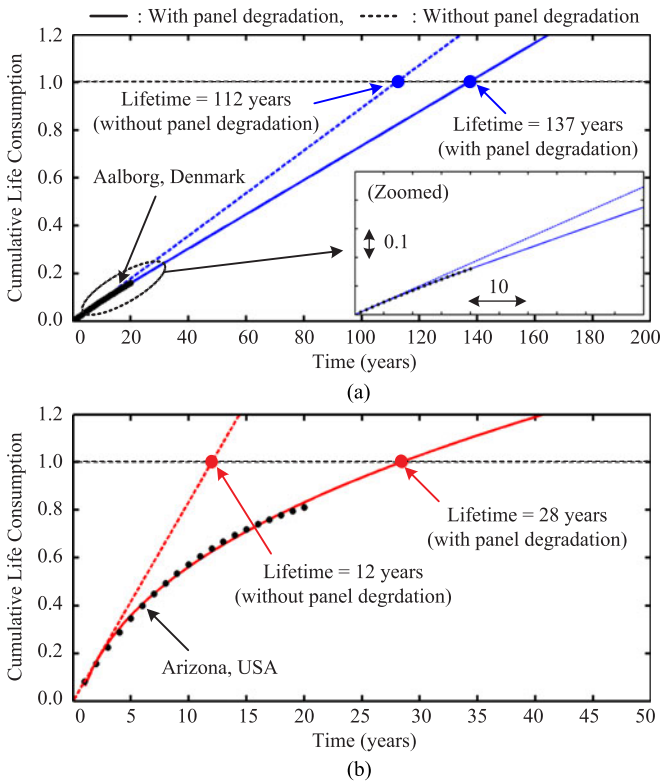

Fig. 9. Cumulative LC of the power device in: (a) Denmark and (b) Arizona. Solid line: with panel degradation, dotted line: without panel degradation.

inverter installed in Arizona reduces significantly during the entire operation, where a reduction of 82% from the initial LC has been observed. In contrast, the LC of the PV inverter in Denmark only reduces by 20% over an operation of 20 years, due to the lower panel degradation rate.

The cumulative LC can then be calculated by accumulating the yearly LC over the entire operation, as it is presented in Fig. 9. In this case, curve fitting is also applied in order to obtain the cumulative LC after an operation of 20 years. The power device is considered to fail when the cumulative LC reaches unity, and the lifetime can then be obtained. According to Fig. 9, the power device of the PV inverter in Denmark and Arizona reaches its end of life after the operations of 137 and 28 years, respectively. It is worth to mention that the cumulative LC in Fig. 9 follows the logarithm function, especially in Arizona. The cumulative LC without considering the degradation rate (linear function) is also shown for comparison, where the estimated lifetime deviates considerably in both cases. Thus, without taking the PV panel degradation into account, the lifetime can be underestimated.

V. Monte Carlo-based Reliability Assessment

From the previous lifetime evaluation, a fixed value of time to failure under a certain operating condition (i.e., the mission profile and the PV panel degradation rate) can be obtained. However, this situation only occurs in an ideal case, where all the power devices fail at the same time. In reality, there are parameter variations, which are mainly introduced by the manufacturing process and the variation in the stresses. Thus, the lifetime is usually expressed in terms of statistical values rather than a fixed value. This can be obtained by means of the Monte Carlo analysis, as illustrated in Fig. 10 [44]–[47].

A. Determination of Equivalent Static Values

In order to apply the Monte Carlo simulation, the parameter variations should be introduced. However, this is not straightforward in the case of stress variations (T_{jm}, ΔT_j, and t_{on}), since these parameters change dynamically and cannot easily be modeled with a distribution function (e.g., a normal distribution). Thus, these dynamic parameters (T_{jm}, ΔT_j, and t_{on}) have to be converted into equivalent static ones (T'_{jm}, $\Delta T'_j$, and t'_{on}), which results in the same lifetime when applying them to the lifetime evaluation process [44], [46].

Actually, there are several possible combinations of equivalent static values that can be applied to achieve a certain lifetime prediction. In order to reduce the degree of freedom in (1), two parameters of the equivalent static values should be fixed. In this regards, t'_{on} is selected to be 0.01 s, which corresponds to the line frequency (i.e., 50 Hz) thermal cycling. Then, the equivalent static mean junction temperature T'_{jm} is calculated from the average value of the mean junction temperature T_{jm} during the entire operation. After that, an equivalent static value of $\Delta T'_j$ can be solved, as it is shown in Table IV.

B. Time-to-Failure Distribution Using Weibull

With the equivalent static values in Table IV, the parameter variations in the lifetime model can be introduced. In this study, 5% variation is applied to all the lifetime model parameters in (1) and also to the equivalent static value of the stress parameters in Table IV, which are modeled by a normal distribution. Then, the Monte Carlo analysis with a population of 10 000 samples is simulated (for each mission profile) with the lifetime model in (1). After that, the lifetime yield for different 10 000 samples can be obtained and fitted with the Weibull distribution, since the lifetime distribution (failure distribution) of the power device $f(x)$ usually follows the Weibull distribution [48], whose probability density function (PDF) can be expressed as

$$f(x) = \frac{\beta}{\eta^{\beta}} x^{\beta-1} \exp\left[-\left(\frac{x}{\eta}\right)^{\beta}\right] \tag{3}$$

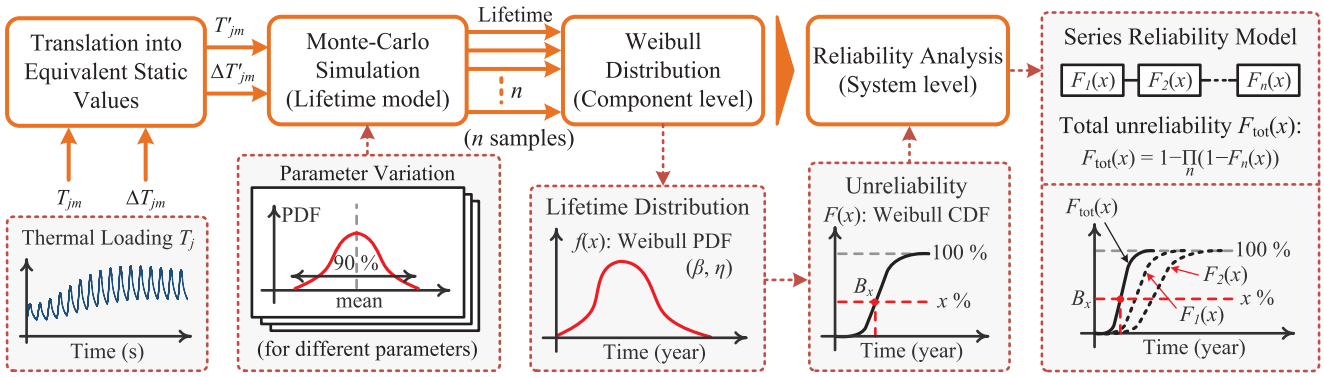

Fig. 10. Flow diagram of the Monte Carlo-based reliability assessment of PV inverters with the reliability block diagram.

TABLE IV
EQUIVALENT STATIC VALUES OF THE STRESS PARAMETERS

Parameters	Denmark	Arizona
Mean junction temperature T'_{jm}	13.45 °C	31.55 °C
Cycle amplitude $\Delta T'_j$	5.69 °C	7.67 °C
Cycle period t'_{on}	0.01 s	
Number of cycles per year n'_i	(365 ×24 × 60× 60) × 50	
Yearly LC	0.0073	0.0356
Lifetime prediction	137 years	28 years

where β is the shape parameter, η is the scale parameter, and x is the operation time. The value of β is normally used for representing a failure mode, as the same failure mode will result in a similar β, whereas the scale parameter η corresponds to the time when 63.2 % of population will have failed [4].

The lifetime distribution obtained from Monte Carlo's simulation with 10 000 samples with the mission profiles in Denmark and Arizona are shown in Figs. 11 and 12, respectively. For each mission profile, two simulation cases with and without considering the PV panel degradation are carried out. It can be seen from the results in Fig. 11 that the PV panel degradation only has a small impact on the lifetime distribution of the PV inverter installed in Denmark, where only a small difference between the lifetime distribution (i.e., Weibull PDF) in Fig. 11(a) and (b) is observed. In contrast, the lifetime distribution of the PV inverter installed in Arizona is significantly affected by the PV panel degradation. It can be seen from Fig. 12(a) that the mean value and the variation in the lifetime distribution is lower in the case when without considering the PV panel degradation. When taking the PV panel degradation into account, both the mean value and the variation in the lifetime of the PV inverter installed in Arizona increase considerably, as it can be seen from the Weibull PDF in Fig. 12(b).

C. Component-Level Reliability Analysis

From the lifetime distribution, the reliability of the power device (e.g., one single component) can be evaluated by considering the cumulative density function (CDF) of the Weibull distribution. This Weibull CDF $F(x)$ is normally referred to as

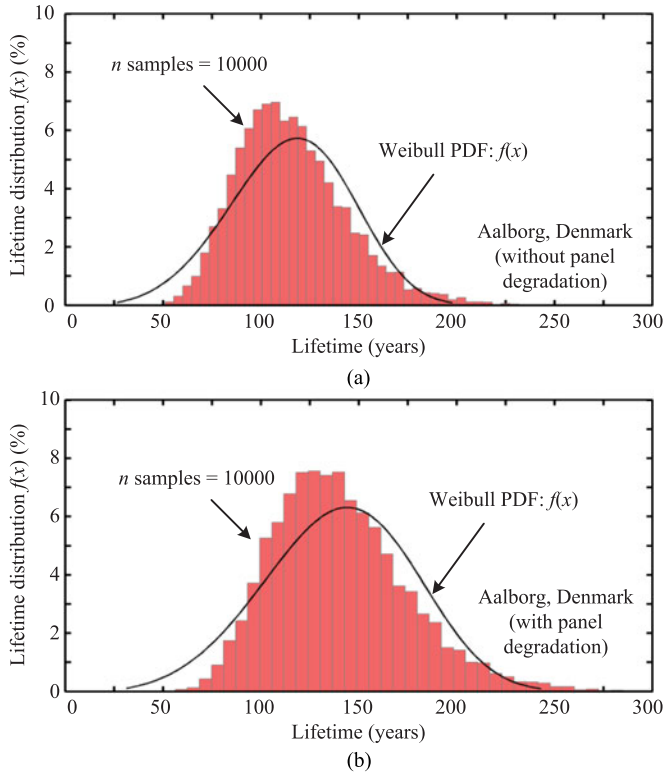

Fig. 11. Lifetime distribution of the PV inverter installed in Denmark (one single power device) obtained from the Monte Carlo simulation with 10 000 samples: (a) without panel degradation and (b) with panel degradation.

the unreliability function, which can be obtained as

$$F(x) = \int_0^x f(x)dx \tag{4}$$

where $f(x)$ is the Weibull distribution and x is the operation time. In general, the unreliability function $F(x)$ represents the proportion of failure population as a function of time. Then, the B_x lifetime, which represents the time when x% of a population is failed, of one power device can be obtained from the unreliability function, and the power device lifetime can be predicted.

Examples of the unreliability functions of the PV inverter installed in Denmark and Arizona (which are constructed based

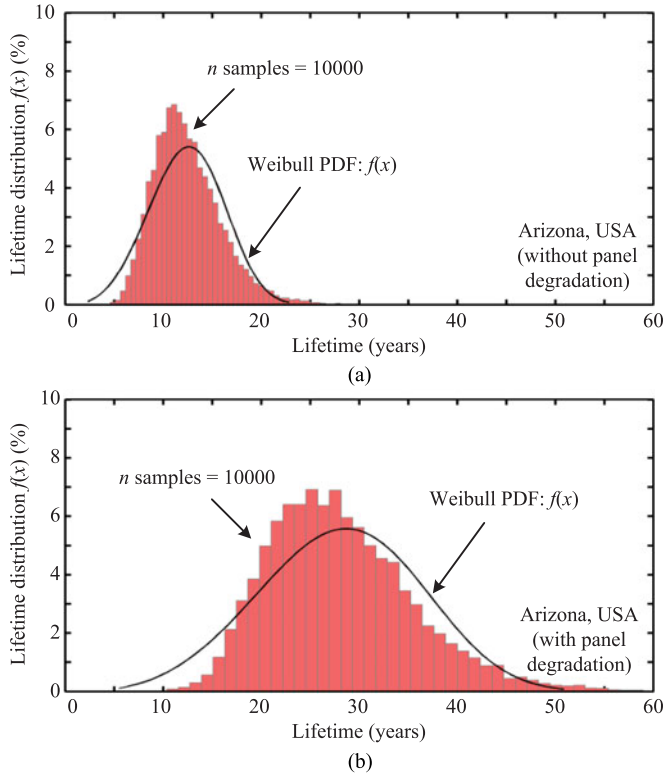

Fig. 12. Lifetime distribution of the PV inverter installed in Arizona (one single power device) obtained from the Monte Carlo simulation with 10 000 samples: (a) without panel degradation and (b) with panel degradation.

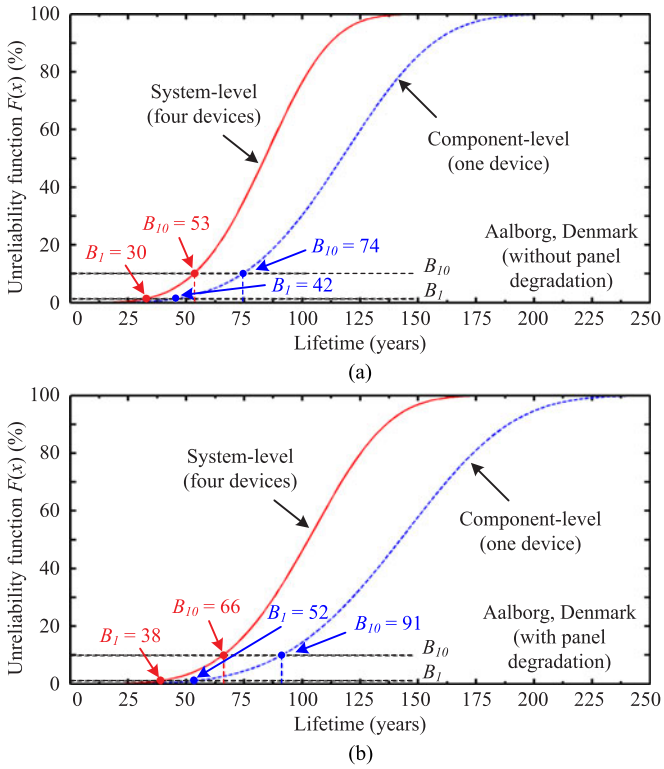

Fig. 13. Unreliability function of the PV inverter installed in Denmark: (a) without panel degradation and (b) with panel degradation, where blue lines indicate component-level and red lines indicate system-level reliability.

on the lifetime distribution in Figs. 10 and 11) are shown in Figs. 12 and 13, respectively. The unreliability function of one power device is indicated by the blue plot together with the B_x lifetime of the power device (e.g., B_1 and B_{10}). For instance, the B_1 and B_{10} lifetime of the power device with the mission profile in Denmark without considering the panel degradation are 42 and 74 years, respectively. This indicates that 1% of the population is expected to fail after an operation of 42 years, whereas 10% of the population is expected to fail after 74 years. When taking the PV panel degradation into account, both the B_1 and B_{10} lifetime of the power device are increased to 52 and 91 years, indicating the impact of the PV panel degradation on the power device lifetime. The impact of panel degradation is even more amplified in the case of the PV inverters installed in Arizona due to the high panel degradation rate, where a significant difference in power device lifetime can be seen as it is summarized in Table V.

TABLE V
LIFETIME EVALUATION RESULTS BASED ON THE MONTE CARLO SIMULATIONS

Operating conditions	Component-level		System-level	
	B_{10}	B_1	B_{10}	B_1
Denmark with panel degradation	91	52	66	38
Denmark without panel degradation	74	42	53	30
Arizona with panel degradation	18	10	13	7
Arizona without panel degradation	8	5	6	3

D. System-Level Reliability Analysis

In order to further obtain a system-level reliability assessment (e.g., PV inverter), a reliability block diagram of the PV inverter needs to be constructed based on the component-level reliability assessment [3], which has been applied to one single power device (e.g., IGBT) in the inverter. Basically, the reliability block diagram is a representative of the reliability interaction between each component in the system. Taking the PV inverter with a full-bridge topology in Fig. 1 as an example, the reliability analysis of the full-bridge inverter can be realized by a series connection of the reliability block diagram in Fig. 10, since the inverter will fail if any of the four devices fails (neglecting the redundancy). Notably, only the reliability of the power devices is taken into account in this study. However, the reliability block diagram can be extended by including other components in the system (e.g., capacitor), which is a subject for future research. Accordingly, the system-level (four devices) unreliability function $F_{\text{tot}}(x)$ can be calculated as

$$F_{\text{tot}}(x) = 1 - \prod_{n=1}^{4} (1 - F_n(x)). \tag{5}$$

In the full-bridge inverter topology [with a bipolar pulse width modulation (PWM) modulation scheme], the thermal loading

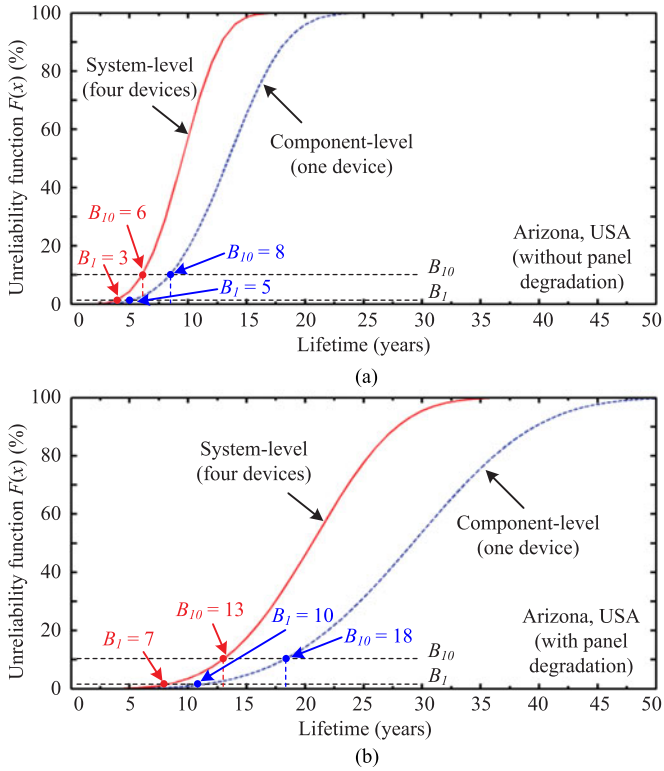

Fig. 14. Unreliability function of the PV inverter installed in Arizona: (a) without panel degradation and (b) with panel degradation, where blue lines indicate component-level and red lines indicate system-level reliability.

of each device is identical (i.e., $F(x) = F_1(x) = F_2(x) = F_3(x) = F_4(x)$). Therefore, the system-level unreliability function can be simplified as $F_{\text{tot}}(x) = 1 - (1 - F(x))^4$.

The system-level unreliability function of four power devices with mission profile in Denmark and Arizona are shown as the red plot in Figs. 13 and 14, respectively. The system-level B_x lifetime is shown in the same figure and also summarized in Table V, where it can be seen that the system-level B_x lifetime differs significantly, similar to that in the component-level lifetime. For instance, the system-level B_{10} lifetime of the PV inverter installed in Arizona is underestimated by 54% (7 years), if the panel degradation is not considered. This means that the PV inverter in the case when without considering panel degradation is expected to be replaced approximately twice as many as the case where the panel degradation is considered. This will inevitably lead to a significant overestimation in the maintenance costs of PV inverters during the entire operation and, thus, the cost of PV energy during the design phase. Similar deviations are also observed in the case of the PV inverters installed in Denmark, where the difference in the system-level B_{10} lifetime is 20% (13 years). In this case, the deviation in the lifetime is relatively smaller due to the lower degradation rate in Denmark, compared to the Arizona case. Nevertheless, it is clear from the results in both installation sites that the panel degradation has a strong impact on the lifetime prediction of the PV inverter, and thus it should be taken into consideration when evaluating the PV inverter lifetime.

VI. Conclusion

The impact of the PV panel degradation on the lifetime evaluation of PV inverters has been presented in this paper. The evaluation is based on the mission profiles with hot climate (i.e., Arizona) and cold climate (i.e., Denmark) conditions, where the degradation rate of the PV panel at the two locations has also been taken into account. The analysis reveals that the thermal loading and the LC of the PV inverters decrease considerably during operation, especially in the hot climate where the PV panel degrades fast. In this condition, the estimated lifetime can be deviated by 54% if the panel degradation is not taken into account. Accordingly, the PV panel degradation has an impact on the lifetime of PV inverter and, thus, has to be considered in the lifetime evaluation and also in the design phase.

References

[1] REN21, "Renewables 2016: Global Status Report (GRS)," 2016. [Online]. Available: http://www.ren21.net/

[2] G. Petrone, G. Spagnuolo, R. Teodorescu, M. Veerachary, and M. Vitelli, "Reliability issues in photovoltaic power processing systems," *IEEE Trans. Ind. Electron.*, vol. 55, no. 7, pp. 2569–2580, Jul. 2008.

[3] Y. Song and B. Wang, "Survey on reliability of power electronic systems," *IEEE Trans. Power Electron.*, vol. 28, no. 1, pp. 591–604, Jan. 2013.

[4] H. S.-H. Chung, H. Wang, F. Blaabjerg, and M. Pecht, *Reliability of Power Electronic Converter Systems*. London, U.K.: IET, 2015.

[5] National Renewable Energy Laboratory, "On the path to sunshot: The role of advancements in solar photovoltaic efficiency, reliability, and costs," U.S. Department of Energy, Washington, DC, USA: Tech. Rep. NREL/TP-6A20-65872, 2016.

[6] A. Golnas, "PV system reliability: An operator's perspective," *IEEE J. Photovolt.*, vol. 3, no. 1, pp. 416–421, Jan. 2013.

[7] C. A. F. Fernandes, J. P. N. Torres, M. Morgado, and J. A. P. Morgado, "Aging of solar PV plants and mitigation of their consequences," in *Proc. IEEE Int. Power Electron. Motion Control Conf.*, Sep. 2016, pp. 1240–1247.

[8] L. M. Moore and H. N. Post, "Five years of operating experience at a large, utility-scale photovoltaic generating plant," *Progress Photovolt., Res. Appl.*, vol. 16, no. 3, pp. 249–259, 2008.

[9] H. Wang, M. Liserre, and F. Blaabjerg, "Toward reliable power electronics: Challenges, design tools, and opportunities," *IEEE Ind. Electron. Mag.*, vol. 7, no. 2, pp. 17–26, Jun. 2013.

[10] H. Huang and P. A. Mawby, "A lifetime estimation technique for voltage source inverters," *IEEE Trans. Power Electron.*, vol. 28, no. 8, pp. 4113–4119, Aug. 2013.

[11] M. Musallam, C. Yin, C. Bailey, and M. Johnson, "Mission profile-based reliability design and real-time life consumption estimation in power electronics," *IEEE Trans. Power Electron.*, vol. 30, no. 5, pp. 2601–2613, May 2015.

[12] M. Andresen, G. Buticchi, and M. Liserre, "Thermal stress analysis and MPPT optimization of photovoltaic systems," *IEEE Trans. Ind. Electron.*, vol. 63, no. 8, pp. 4889–4898, Aug. 2016.

[13] A. Anurag, Y. Yang, and F. Blaabjerg, "Thermal performance and reliability analysis of single-phase PV inverters with reactive power injection outside feed-in operating hours," *IEEE Trans. Emerg. Sel. Topics Power Electron.*, vol. 3, no. 4, pp. 870–880, Dec. 2015.

[14] Y. Yang, H. Wang, and F. Blaabjerg, "Improved reliability of single-phase PV inverters by limiting the maximum feed-in power," in *Proc. IEEE Energy Convers. Congr. Expo.*, Sep. 2014, pp. 128–135.

[15] Y. Yang, E. Koutroulis, A. Sangwongwanich, and F. Blaabjerg, "Minimizing the levelized cost of energy in single-phase photovoltaic systems with an absolute active power control," *IEEE Ind. Appl. Mag.*, vol. 23, no. 5, pp. 1–10, Sep./Oct. 2017.

[16] S. E. D. Leon-Aldaco, H. Calleja, F. Chan, and H. R. Jimenez-Grajales, "Effect of the mission profile on the reliability of a power converter aimed at photovoltaic applications—A case study," *IEEE Trans. Power Electron.*, vol. 28, no. 6, pp. 2998–3007, Jun. 2013.

[17] N. C. Sintamarean, F. Blaabjerg, H. Wang, F. Iannuzzo, and P. de Place Rimmen, "Reliability oriented design tool for the new generation of grid

connected PV-inverters," *IEEE Trans. Power Electron.*, vol. 30, no. 5, pp. 2635–2644, May 2015.
[18] A. Anurag, Y. Yang, and F. Blaabjerg, "Reliability analysis of single-phase PV inverters with reactive power injection at night considering mission profiles," in *Proc. IEEE Energy Convers. Congr. Expo.*, Sep. 2015, pp. 2132–2139.
[19] C. Felgemacher, S. Araujo, C. Noeding, P. Zacharias, A. Ehrlich, and M. Schidleja, "Evaluation of cycling stress imposed on IGBT modules in PV central inverters in sunbelt regions," in *Proc. Int. Conf. Integr. Power Electron. Syst.*, Mar. 2016, pp. 1–6.
[20] Y. Yang, H. Wang, F. Blaabjerg, and K. Ma, "Mission profile based multi-disciplinary analysis of power modules in single-phase transformerless photovoltaic inverters," in *Proc. Eur. Conf. Power Electron. Appl.*, Sep. 2013, pp. 1–10.
[21] E. L. Meyer and E. E. van Dyk, "Assessing the reliability and degradation of photovoltaic module performance parameters," *IEEE Trans. Rel.*, vol. 53, no. 1, pp. 83–92, Mar. 2004.
[22] M. Vazquez and I. Rey-Stolle, "Photovoltaic module reliability model based on field degradation studies," *Progress Photovolt., Res. Appl.*, vol. 16, no. 5, pp. 419–433, 2008.
[23] V. Sharma and S. Chandel, "Performance and degradation analysis for long term reliability of solar photovoltaic systems: A review," *Renewable Sustain. Energy Rev.*, vol. 27, pp. 753–767, 2013.
[24] D. C. Jordan and S. R. Kurtz, "Photovoltaic degradation rates—An analytical review," *Progress Photovolt., Res. Appl.*, vol. 21, no. 1, pp. 12–29, 2013.
[25] D. C. Jordan, J. H. Wohlgemuth, and S. R. Kurtz, "Technology and climate trends in PV module degradation," in *Proc. Eur. PV Solar Energy Conf.*, Sep. 2012, pp. 3118–3124.
[26] D. C. Jordan, S. R. Kurtz, K. VanSant, and J. Newmiller, "Compendium of photovoltaic degradation rates," *Progress Photovolt., Res. Appl.*, vol. 24, no. 7, pp. 978–989, 2016.
[27] M. Köntges, S. Altmann, T. Heimberg, U. Jahn, and K. A. Berger, "Mean degradation rates in pv systems for various kinds of PV module failures," in *Proc. Eur. PV Solar Energy Conf.*, Jun. 2016, pp. 1435–1443.
[28] K. J. Sauer, "Real-world challenges and opportunities in degradation rate analysis for commercial PV systems," in *Proc. IEEE Photovolt. Spec. Conf.*, Jun. 2011, pp. 003208–003212.
[29] J. Hedström and L. Palmblad, "Performance of old PV modules: measurement of 25 years old crystalline silicon modules," *Elforsk Rapport 06*, vol. 71, pp. 1–14, 2006.
[30] Y. Tang, B. Raghuraman, J. Kuitche, G. TamizhMani, C. E. Backus, and C. Osterwald, "An evaluation of 27+ years old photovoltaic modules operated in a hot-desert climatic condition," in *Proc. 4th World Conf. Photovolt. Energy Convers.*, May 2006, vol. 2, pp. 2145–2147.
[31] S. Spataru, P. Cernek, D. Sera, T. Kerekes, and R. Teodorescu, "Characterization of a crystalline silicon photovoltaic system after 15 years of operation in northern Denmark," in *Proc. Eur. PV Solar Energy Conf.*, 2014, pp. 2680–2688.
[32] A. Sangwongwanich, Y. Yang, D. Sera, and F. Blaabjerg, "Lifetime evaluation of PV inverters considering panel degradation rates and installation sites," in *Proc. IEEE Appl. Power Electron. Conf. Expo.*, Mar. 2017, pp. 1–8.
[33] BPSolar. BP 365, 65 watt photovoltaic module, 2003. Online. [Available]. Available: http://www.solarpanelstore.com/pdf/bp-365.pdf
[34] S.B.Kjaer, J.K.Pedersen, and F. Blaabjerg, "A review of single-phase grid-connected inverters for photovoltaic modules," *IEEE Trans. Ind. Appl.*, vol. 41, no. 5, pp. 1292–1306, Sep. 2005.
[35] *Infineon Technologies AG*, SGP30N60, München, Germany, 2007, rev. 2.3.
[36] S. Kouro, J. I. Leon, D. Vinnikov, and L. G. Franquelo, "Grid-connected photovoltaic systems: An overview of recent research and emerging PV converter technology," *IEEE Ind. Electron. Mag.*, vol. 9, no. 1, pp. 47–61, Mar. 2015.
[37] F. Blaabjerg, R. Teodorescu, M. Liserre, and A.V.Timbus, "Overview of control and grid synchronization for distributed power generation systems," *IEEE Trans. Ind. Electron.*, vol. 53, no. 5, pp. 1398–1409, Oct. 2006.
[38] D. C. Jordan, T. J. Silverman, B. Sekulic, and S. R. Kurtz, "PV degradation curves: Non-linearities and failure modes," *Progress Photovolt., Res. Appl.*, pp. 1–9, 2016.
[39] C. R. Osterwald, J. Adelstein, J. A. d. Cueto, B. Kroposki, D. Trudell, and T. Moriarty, "Comparison of degradation rates of individual modules held at maximum power," in *Proc. 4th World Conf. Photovolt. Energy Convers.*, May 2006, vol. 2, pp. 2085–2088.
[40] E. Collins *et al.*, "A reliability and availability sensitivity study of a large photovoltaic system," in *Proc. Eur. PV Solar Energy Conf.*, 2010, pp. 4463–4469.
[41] F. He, Z. Zhao, and L. Yuan, "Impact of inverter configuration on energy cost of grid-connected photovoltaic systems," *Renewable Energy*, vol. 41, pp. 328–335, 2012.
[42] D. Sera, R. Teodorescu, and P. Rodriguez, "PV panel model based on datasheet values," in *Proc. IEEE Int. Symp. Ind. Electron.*, Jun. 2007, pp. 2392–2396.
[43] U. Scheuermann, R. Schmidt, and P. Newman, "Power cycling testing with different load pulse durations," in *Proc. Int. Conf. Power Electron., Mach. Drives*, Apr. 2014, pp. 1–6.
[44] P. D. Reigosa, H. Wang, Y. Yang, and F. Blaabjerg, "Prediction of bond wire fatigue of IGBTs in a PV inverter under a long-term operation," *IEEE Trans. Power Electron.*, vol. 31, no. 10, pp. 7171–7182, Oct. 2016.
[45] Y. Shen, H. Wang, Y. Yang, P. D. Reigosa, and F. Blaabjerg, "Mission profile based sizing of IGBT chip area for PV inverter applications," in *Proc. Int. Symp. Power Electron. Distrib. Gen. Syst.*, Jun. 2016, pp. 1–8.
[46] D. Zhou, H. Wang, F. Blaabjerg, S. K. Kaer, and D. Blom-Hansen, "System-level reliability assessment of power stage in fuel cell application," in *Proc. IEEE Energy Convers. Congr. Expo.*, Sep. 2016, pp. 1–8.
[47] K. Ma, H. Wang, and F. Blaabjerg, "New approaches to reliability assessment: Using physics-of-failure for prediction and design in power electronics systems," *IEEE Power Electron. Mag.*, vol. 3, no. 4, pp. 28–41, Dec. 2016.
[48] ZVEI, "How to measure lifetime for robustnesss validation–step by step," Berlin, Germany, rev. 1.9, Nov. 2012.

Ariya Sangwongwanich (S'15) received the B.Eng. degree in electrical engineering from Chulalongkorn University, Bangkok, Thailand, in 2013, and the M.Sc. degree in energy engineering from Aalborg University, Aalborg, Denmark, in 2015, where he is currently working toward the Ph.D. degree.

His research interests include control of grid-connected converter, photovoltaic systems, reliability in power electronics, and high-power multilevel converters.

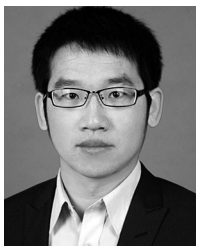

Yongheng Yang (S'12–M'15) received the B.Eng. in electrical engineering degree from Northwestern Polytechnical University, Xi'an, China, in 2009, and the Ph.D. degree in electrical engineering from Aalborg University, Aalborg, Denmark, in 2014.

He was a Postgraduate with Southeast University, China, from 2009 to 2011. In 2013, he was a Visiting Scholar with Texas A&M University, College Station, TX, USA. Since 2014, he has been with the Department of Energy Technology, Aalborg University, where he is currently an Assistant Professor. He has published more than 80 technical papers and coauthored a book—*Periodic Control of Power Electronic Converters* (London, UK: IET). His research interests include grid integration of renewable energy systems, power converter design, analysis and control, harmonics identification and mitigation, and reliability in power electronics.

Dr. Yang is a member of the IEEE Power Electronics Society (PELS) Students and Young Professionals Committee. He was a Guest Associate Editor of the IEEE JOURNAL OF EMERGING AND SELECTED TOPICS IN POWER ELECTRONICS and a Guest Editor of *Applied Sciences*. He is an active reviewer for relevant top-tier journals.

Dezso Sera (S'05–M'08–SM'15) received the B.Sc. and M.Sc. degrees in electrical engineering from the Technical University of Cluj, Cluj-Napoca, Romania, in 2001 and 2002, respectively, the M.Sc. degree in power electronics and the Ph.D. degree in PV systems from the Department of Energy Technology, Aalborg University, Aalborg, Denmark, where he is currently an Associate Professor.

Since 2009, he has been Programme Leader of the Photovoltaic Systems Research Programme (www.pv-systems.et.aau.dk) at the same department. His research interests include modeling, characterization, diagnostics and maximum power point tracking (MPPT) of PV arrays, as well as power electronics, and grid integration for PV systems.

Frede Blaabjerg (S'86–M'88–SM'97–F'03) was with ABB-Scandia, Randers, Denmark, from 1987 to 1988. From 1988 to 1992, he was a Ph.D. degree in electrical engineering student with Aalborg University, Aalborg, Denmark, in 1995.

He became an Assistant Professor in 1992, Associate Professor in 1996, and Full Professor of power electronics and drives in 1998. His current research interest focuses on power electronics and its applications such as in wind turbines, PV systems, reliability, harmonics, and adjustable speed drives.

Dr. Blaabjerg received the 18 IEEE Prize Paper Awards, the IEEE PELS Distinguished Service Award in 2009, the EPE-PEMC Council Award in 2010, the IEEE William E. Newell Power Electronics Award 2014, and the Villum Kann Rasmussen Research Award 2014. He was the Editor-in-Chief of the IEEE TRANSACTIONS ON POWER ELECTRONICS from 2006 to 2012. He was nominated in 2014, 2015, and 2016 by Thomson Reuters to be between the most 250 cited researchers in Engineering in the world.